JACS
JOURNAL OF THE AMERICAN CHEMICAL SOCIETY

COMMUNICATION

pubs.acs.org/JACS

Real-Time Monitoring of Surface-Initiated Atom Transfer Radical Polymerization Using Silicon Photonic Microring Resonators: Implications for Combinatorial Screening of Polymer Brush Growth Conditions

F. Ted Limpoco and Ryan C. Bailey*

Department of Chemistry, University of Illinois at Urbana−Champaign, 600 South Mathews Avenue, Urbana, Illinois 61801, United States

Supporting Information

ABSTRACT: We directly monitor in parallel and in real time the temporal profiles of polymer brushes simultaneously grown via multiple ATRP reaction conditions on a single substrate using arrays of silicon photonic microring resonators. In addition to probing relative polymerization rates, we show the ability to evaluate the dynamic properties of the *in situ* grown polymers. This presents a powerful new platform for studying modified interfaces that may allow for the combinatorial optimization of surface-initiated polymerization conditions.

Direct polymerization on surfaces via surface-bound initiators is an established mode of creating polymer brushes and modifying their interfacial properties. Many polymerization technologies have been employed, as well as surface-sensitive techniques that interrogate brush composition, thickness, topography, wetting, and viscoelastic properties.[1] Very few, however, are able to track actual brush growth on the surface. Here we describe real-time monitoring of polymer brush growth from the surface of a silicon-based photonic sensor and its utility in the combinatorial screening of growth conditions. Moreover, all stages of surface modification can be tracked *in situ*, from installation of initiators to polymer growth, as well as characterization of the interfacial properties of the final polymer product. In this case, we are able to quantify the amount of serum proteins irreversibly adsorbed on the polymer brush surface, indicating its performance as an anti-biofouling coating.

The sensor platform consists of arrays of micrometer-sized ring-shaped optical waveguides etched into a silicon-on-insulator (SOI) chip (Figure 1a). These microring resonators are high-finesse microcavity devices that resonantly confine specific wavelengths of light according to an interferometric-based condition: $m\lambda = 2\pi r n_{eff}$, where m is an integer, λ is the wavelength of light, r is the radius of the cavity, and n_{eff} is the effective refractive index of the optical mode.[2] The attachment of molecular species to the surface of the sensor modulates the effective refractive index, and this effect is transduced as a shift in the resonance wavelengths supported by the cavity. The system's high refractive index contrast makes it exceedingly surface sensitive, allowing for observation of polymerization in the presence of high monomer concentrations. This type of sensor, which is afforded scalability and multiplexing capability due to well-established methods of semiconductor fabrication, has been exploited by our group for several biosensing applications.[3−8] Here we show that polymerization off of the resonator surface can be probed by measuring shifts in resonance wavelength, allowing direct and continuous monitoring of the growth kinetics of surface-initiated polymerization (SIP), as illustrated in Figure 1.

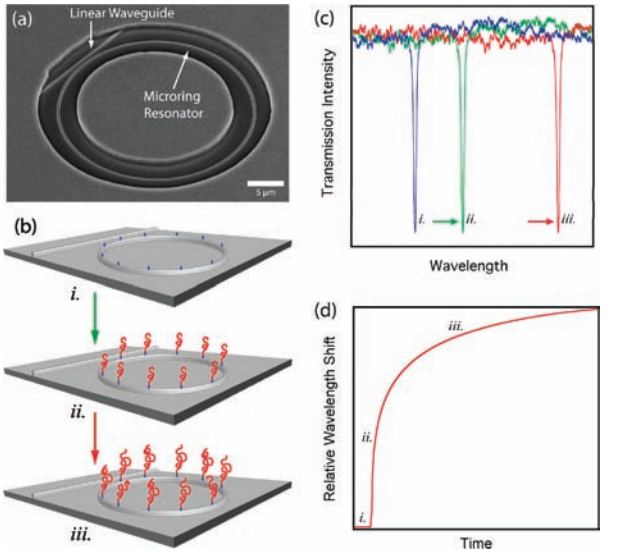

Figure 1. (a) Scanning electron micrograph of an individual microring and adjacent linear waveguide on a silicon-on-insulator chip, exposed to solution through an annular opening in a fluoropolymer cladding layer. (b) Surface polymerization is performed by first functionalizing the rings with initiator followed by exposure to the monomer/catalyst solution. (c) Resonant optical modes supported on the microring are extremely sensitive to changes in the local dielectric environment, shifting to longer wavelengths as polymerization occurs. (d) The shifts in resonance wavelength can be monitored in real time, allowing relative rates of surface-initiated polymerization to be directly observed.

Polymers attached to surfaces can form brush-like structures known to impart interesting physical behaviors,[1] such as responsiveness to pH,[9] ionic strength,[10] temperature,[11] and solvent quality,[12] and confer useful properties in terms of adhesion,[13] lubrication,[14] viscoelasticity,[15] wettability,[16] and fouling resistance at interfaces.[17] Poly(ethylene glycol) (PEG) brushes, for example,

Received: June 9, 2011
Published: September 07, 2011

are known to be highly stretched in aqueous solvents, producing lubricious surfaces that are also resistant to protein adsorption; this is mainly due to entropically driven repulsive forces manifested from their high retention of water in extended form.[18,19] Zwitterionic polymer brushes, such as poly(sulfobetaine methacrylate) (pSBMA), have been shown to exhibit similar, if not superior, antibiofouling properties for the same reason; in this case, ionic solvation produces high retention of water, compared to extensive hydrogen bond formation in the case of PEG-based systems.[20,21]

Atom transfer radical polymerization (ATRP) has emerged as the most common method of implementing controlled polymer growth on surfaces.[1] Typically, ATRP is initiated with the abstraction of a labile halogen (e.g., from an α-bromoester) by a metal−ligand catalyst complex (e.g., Cu^+ and 2,2′-bipyridyl) via homolytic cleavage, generating an active radical moiety to which monomers (e.g., methacrylates) can be added.[22] Control is imposed on the chain reaction by rapid deactivation of the radical and subsequent equilibria between the inactive and active forms. This produces the characteristic features of "controlled" and "living" polymerizations in solution, i.e., linear conversion, high turnovers, low polydispersity, and the ability to prepare block copolymers by stopping and restarting polymerization.

Continuous monitoring of surface polymerization has been performed on the quartz crystal microbalance (QCM), which utilizes a quartz crystal mechanical resonator to detect mass loading due to polymer growth as a negative shift in resonance frequency;[15,23,24] however, uncertain viscoelastic effects can complicate the interpretation of QCM data. Not many methods directly observe the growth of polymer brushes, and even fewer are amenable to even a modest throughput in screening growth conditions (e.g., QCM can only monitor a single reaction at a time). ATRP, for example, requires multiple parameters to be optimized in order to achieve controlled growth. The degree of control is determined by the position of the equilibria and can be tuned by the proper selection of metals, halogens, ligands, and solvents. The sensitivity of silicon photonic microrings to changes in optical density on their surfaces makes them potentially useful in the direct and continuous monitoring of SI-ATRP from real-time shifts in resonance wavelengths, and the multiplexing capability that is freely available when using an array of individually addressable sensors presents an intriguing method to combinatorially screen multiple reaction conditions *in situ*.

The chemical functionalization and polymerization chemistry to grow polymer brushes on microring resonators is shown in the Supporting Information. The surfaces were first functionalized with 11-(2-bromo-2-methylpropionyloxy)undecyltrichlorosilane (BMPOUTS), an ATRP initiator consisting of an α-bromoester moiety that can be tethered onto the oxide layer of the silicon surface via chlorosilane chemistry.

A microring resonator array sensor chip, having 32 sensors, was fitted with a two-channel microfluidic gasket to selectively functionalize 12 active microrings with the BMPOUTS (test rings), leaving another 12 active, but nonfunctionalized, and thus able to be used as control rings during the polymerization. The final 8 microrings are obscured from the solution by a fluoropolymer cladding layer and used to correct for thermal drift (reference rings) during the experiment. Initiator immobilization was followed in real time, and the resonance wavelength shift from only the sensors exposed to BMPOUTS confirmed selective functionalization. The chip was sonicated in hexane to remove any physisorbed material and reloaded into a microfluidic chamber that allowed subsequent solutions to be flowed

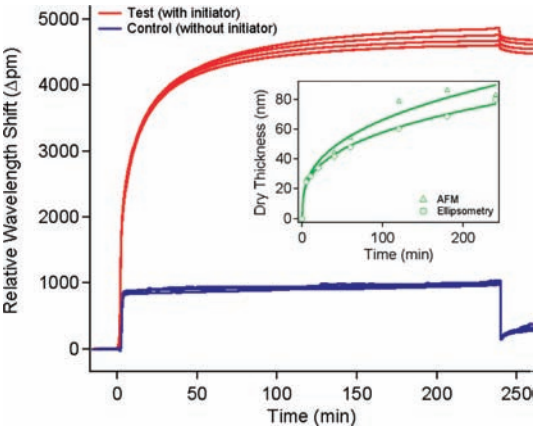

Figure 2. Real-time shifts in resonance wavelength of an array of eight microrings (four tests and four controls). At t = 0 min, the solution was switched from degassed solvent (50:50 methanol:water) to a monomer/catalyst solution (0.38 M SBMA, 0.1 M PMDETA, and 0.1 M CuBr), and back to the solvent at t = 240 min. The growth of polymer from microrings functionalized with the ATRP initiator (red) is clearly observed in comparison to those left nonfunctionalized (blue), which are only sensitive to differences in the bulk refractive index between the two solutions. Inset: Dry thickness of pSBMA grown on bulk silicon wafers as a function of polymerization time, as determined via AFM and ellipsometry.

over the entire array of active sensors. Polymerization was accomplished by flowing degassed solvent (50:50 methanol:water) to achieve a stable baseline before introducing the monomer/catalyst solution (0.38 M SBMA, 0.1 M PMDETA, 0.1 M CuBr) for 4 h and terminating with a solvent wash.

The real-time shifts in resonance wavelength for four representative test and four control microrings as the monomer/catalyst solution was flowed over the array are shown in Figure 2. Clearly polymerization occurred on the test channel, which showed a progressive increase in resonance shift over time, and not on the control channel, which exhibited a single-point jump associated with the difference in bulk refractive index between the solvent and monomer/catalyst solution. This bulk refractive index shift is also measured by the test rings, but this occurs simultaneously with rapid polymer growth. Replacing the monomer/catalyst solution with the original solvent results in the control rings dropping back toward zero net shift, consistent with a reversal in the bulk index shift, while the test channel retains a large resonance shift of ∼4500 pm. The reversed bulk index shift is smaller for the test rings as compared to the control rings, because the physical volume of the grown polymer reduces the amount of bulk solution probed by the evanescent optical field extending from the sensor. The residual shift in the control channel upon switching back to solvent is most likely the tailing of the monomer/catalyst solution from the microfluidic channel, an effect that again is suppressed by the polymer grown on the test rings. Topographic AFM images of individual microrings (see Supporting Information) confirm selective growth of polymer on the test sensors, as opposed to the control microrings.

Focusing just on the initiator-functionalized test rings (red in Figure 2), it is clear that the polymer brush grows rapidly during the first 50 min of exposure to the monomer/catalyst solution, and the growth rate slows significantly over the next 3 h. Purely solution-phase ATRP typically exhibits a linear conversion profile characteristic of controlled radical polymerization systems where an equilibrium is maintained between the active and

deactivated forms of the growing radical chain. However, it was previously shown that surface-immobilized ATRP of acrylates and methacrylates exhibits initial rapid growth, followed by a decline after about 60 min, attributed to the importance of termination events (e.g., radical disproportionation, or coupling) in SIP, since the number of initiators is limited to those tethered on the surface, as compared to increased initiator concentrations in solution.[25−27] Our observation of fast initial growth from the microrings followed by a decrease in polymerization rate after 50 min is consistent with this earlier report.[26]

In addition to monitoring the actual polymerization, silicon photonic microring resonators allow for probing the dynamic chemical or biomolecular properties of derivatized interfaces. The pSBMA polymer investigated herein has been demonstrated to convey anti-biofouling properties to surfaces, and we probed this property in comparison to the adsorption of serum proteins onto both bare oxide-passivated silicon and a poly(L-lysine)-poly(ethyleneglycol) (PLL-PEG)-modified surface. These studies (see Supporting Information) verified the superior resistance of pSBMA coatings toward biofouling of undiluted fetal bovine serum. Beyond the qualitative evaluation of biofouling resistance, we also used an established relationship between bound mass per unit area and resonance wavelength shift[2] to enumerate the amount of nonspecifically adhered serum proteins by measuring the residual shift after returning to buffer solution, finding that pSBMA had 260 pg/mm^2, consistent with previous studies by Jiang and co-workers.[20] By comparison, PLL-*g*-PEG and non-modified surfaces were fouled to extents of 1400 pg/mm^2 and 3000 pg/mm^2, respectively.

Returning to the growth profile of polymerization, we conducted identical polymerizations of pSBMA on native oxide passivated silicon wafers for variable times and analyzed the resultant thickness of the polymer films via ellipsometry and AFM (Figure 2, inset). The *ex situ* ellipsometric and AFM values were measured on dry polymer films, in contrast to the *in situ* microring measurements, which probe the polymer optical density under solvent-swollen conditions, complicating direct comparison of film thicknesses. It is clear that both methods confirm polymer growth under these reaction conditions. Interestingly, though, the growth profiles are not identical, the *ex situ* measurements showing a more gradual decline in polymer growth rate than observed *in situ* using microring resonators. Furthermore, the *ex situ* polymerized brushes are still clearly growing after 4 h of polymerization, whereas the *in situ* microring response appears to plateau, consistent with chain termination. We attribute this difference to the fact that the *in situ* polymerizations were performed in the presence of flow, as opposed to the static ATRP used in the bulk, *ex situ* polymerizations. It was previously shown that agitation of the monomer solution during SIP results in a lower limiting thickness (by ∼50%) on account of enhanced mobility of the chain ends, increasing the likelihood of radical coupling.[26]

An additional consideration in the growth profile measured *in situ* is the evanescent optical field that extends from the sensor, which decays exponentially from the surface of the microring. The spatial profile of the field, which is directly responsible for the device's sensitivity to refractive index changes, is commonly expressed in terms of the 1/*e* decay constant (the distance at which the field has dropped to 36.7%). Previously, we empirically determined the 1/*e* value of our SOI microring resonators to be ∼63 nm, using a layer-by-layer polyelectrolyte multilayer growth approach.[2] The *ex situ* measurements of polymer brush thickness show that this distance is not reached until after very long polymerization times, and thus we suggest that the slowing of the ATRP growth profile after the first 50 min is a consequence of flow-induced chain termination, as opposed to an artifact imposed by the diminishing evanescent sensitivity to polymerization.

Solution flow is required for sustained polymerizations in the microring resonator system, as monomer solutions can be quickly consumed in the small-volume microfluidic environments probed in each experiment. Therefore, it may be difficult to precisely correlate *in situ* growth profiles and/or extract exact polymer brush thicknesses for similar brushes grown *ex situ*, although this is a goal toward which we are currently working. However, the *in situ* platform offers several attractive attributes for optimization of SIP conditions. As for the growth profile shown in Figure 1, the real-time response of the microrings follows a single, continuous polymerization, taking only 4 h to complete and providing a measurement made in the presence of solvent. This is in contrast to typical *ex situ* measurements that often require many separate, specific time-terminated polymerizations, each prone to slight variations in solution composition, followed by many serial measurements of (usually) dry polymer films using ellipsometry. Most importantly, though, the SOI microring resonator platform is highly amenable to on-chip multiplexing, and we believe that arrays of sensors will be extremely useful in parallel screening of reaction conditions to optimize particular properties of a given polymerization method. For example, shifts in resonance wavelengths from arrays of sensors differentially functionalized with unique initiators or exposed to dissimilar reaction conditions (solvent composition, monomer identity and/or concentration, catalyst identity and/or concentration, etc.) could be monitored simultaneously, and variances in relative growth rates would provide a diagnostic comparison of multiple conditions in a single shot.

To demonstrate the ability to efficiently screen different ATRP reactions under distinct conditions in parallel and on a single sensor substrate, we used an array of microring resonators to probe the effects of different catalyst conditions on the growth of pSBMA using the BMPOUTS initiator described above. This configuration removes potential variations in initiator film formation, which is especially advantageous for silane-based systems that are more difficult to precisely control when compared with thiol attachment to gold substrates. Four deoxygenated monomer/catalyst solutions, each consisting of 0.38 M SBMA in 70:30 2-propanol:water, but with unique metal/ligand conditions, were prepared to screen for the effects of ligand type (bpy vs PMDETA), counterion (bromide vs chloride), and the presence or absence of Cu(II). A four-channel microfluidic gasket was fit to a BMPOUTS-modified sensor array, and the four unique monomer/catalyst combinations were simultaneously flowed across different regions of the sensor array before returning to the background solvent.

Real-time shifts in resonance wavelengths for one representative microring exposed to each of the four reaction conditions are shown in Figure 3. The plot clearly shows that the microring resonator platform provides a quick relative assessment of different polymerization conditions, as each condition gives a different growth profile. For example, addition of Cu(II) in a 1:1 molar ratio of $CuBr_2$ and CuBr (red trace in Figure 3) increases the amount of total polymerization compared to the Cu(I)-only condition (blue trace in Figure 3), even with the same total moles of copper ion in solution. This observation is supported by the fact that Cu(II) pushes the equilibria toward the deactivated form of the radical, which decreases the termination rate and results in

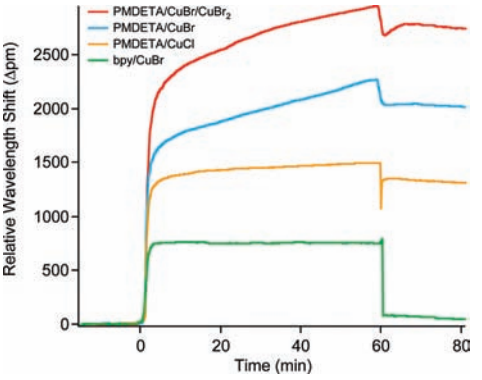

Figure 3. Real-time shifts in the resonance wavelengths of an array of microring resonators simultaneously probing the effects of four different catalyst/ligand combinations in the polymerization of pSBMA.

a thicker polymer brush. We also observe that the amount of polymerization is reduced when CuBr is switched for CuCl, consistent with the previously observed slower deactivation rate for chloride-based systems as compared to when bromide is the anion.[28] We also notice that trading the ligand of PMDETA for bpy results in significantly less polymer growth, a consequence of the bpy system having a ~10-fold lower activation rate constant.[29] In fact, polymerization in the bpy/CuBr system was visible only after returning to the pure solvent, as there was a small residual resonance wavelength shift obscured by the instantaneous bulk index shift at the beginning of the polymerization.

ATRP and other polymerization approaches that can be applied to surfaces are incredibly enabling substrate functionalization methods, allowing a wide range of different chemical or biomolecular properties to be imparted onto surfaces for many highly relevant industrial applications. Many parameters and combinations of parameters influence polymerization, so the search for moderately high throughput approaches to screen for optimal reaction conditions is an important pursuit. Herein we have demonstrated the utility of multiplexed arrays of silicon photonic microring resonators to directly monitor *in situ* the time-dependent growth profile of pSBMA polymer brushes produced using ATRP. Beyond simply establishing that this technology can be used to follow polymerization, we have demonstrated the ability to differentially monitor multiple reaction conditions in parallel and qualitatively observe differences in growth curves that can be explained on the basis of previous observations of ATRP in solution. We have also shown that the same analytical platform can be used to evaluate functional properties of the polymer brushes *in situ*, in this case the antibiofouling properties of pSBMA, and we imagine that we could extend this methodology to follow different volume transitions that occur in response to changes in pH, ionic strength, temperature, or solvent composition. We hope to develop more quantitative models of real-time polymerization from our sensor surfaces to make this a broadly useful technology for optimizing surface polymerization for many applications.

■ ASSOCIATED CONTENT

Supporting Information. Experimental details and characterization data. This material is available free of charge via the Internet at http://pubs.acs.org.

■ AUTHOR INFORMATION

Corresponding Author
baileyrc@illinois.edu

■ ACKNOWLEDGMENT

We acknowledge financial support from the NIH Director's New Innovator Award Program, part of the NIH Roadmap for Medical Research, through grant no. 1-DP2-OD002190-01, and the Roy J. Carver Charitable Trust. We also thank Rick Haasch of the Center for Microanalysis of Materials, Frederick Seitz Materials Research Laboratory, for assistance in XPS measurements, and Ji-Yeon Byeon for the SEM micrograph of the microring resonator in Figure 1a.

■ REFERENCES

(1) Barbey, R.; Lavanant, L.; Paripovic, D.; Schuwer, N.; Sugnaux, C.; Tugulu, S.; Klok, H. A. *Chem. Rev.* **2009**, *109*, 5437.
(2) Luchansky, M. S.; Washburn, A. L.; Martin, T. A.; Iqbal, M.; Gunn, L. C.; Bailey, R. C. *Biosens. Bioelectron.* **2010**, *26*, 1283.
(3) Byeon, J.-Y.; Bailey, R. C. *Analyst* **2011**, *136*, 3430.
(4) Byeon, J.-Y.; Limpoco, F. T.; Bailey, R. C. *Langmuir* **2010**, *26*, 15430.
(5) Luchansky, M. S.; Bailey, R. C. *Anal. Chem.* **2010**, *82*, 1975.
(6) Qavi, A. J.; Bailey, R. C. *Angew. Chem., Int. Ed.* **2010**, *49*, 4608.
(7) Washburn, A. L.; Gunn, L. C.; Bailey, R. C. *Anal. Chem.* **2009**, *81*, 9499.
(8) Washburn, A. L.; Luchansky, M. S.; Bowman, A. L.; Bailey, R. C. *Anal. Chem.* **2010**, *82*, 69.
(9) Wu, T.; Gong, P.; Szleifer, I.; Vlček, P.; Šubr, V.; Genzer, J. *Macromolecules* **2007**, *40*, 8756.
(10) Biesalski, M.; Rühe, J. *Macromolecules* **2004**, *37*, 2196.
(11) LeMieux, M. C.; Peleshanko, S.; Anderson, K. D.; Tsukruk, V. V. *Langmuir* **2007**, *23*, 265.
(12) Brittain, W. J.; Boyes, S. G.; Granville, A. M.; Baum, M.; Mirous, B. K.; Akgun, B.; Zhao, B.; Blickle, C.; Foster, M. D. *Adv. Polym. Sci.* **2006**, *198*, 125.
(13) LeMieux, M. C.; Lin, Y.-H.; Cuong, P. D.; Ahn, H.-S.; Zubarev, E. R.; Tsukruk, V. V. *Adv. Funct. Mater.* **2005**, *15*, 1529.
(14) Limpoco, F. T.; Advincula, R. C.; Perry, S. S. *Langmuir* **2007**, *23*, 12196.
(15) Moya, S. E.; Brown, A. A.; Azzaroni, O.; Huck, W. T. S. *Macromol. Rapid Commun.* **2005**, *26*, 1117.
(16) Uhlmann, P.; Ionov, L.; Houbenov, N.; Nitschke, M.; Grundke, K.; Motornov, M.; Minko, S.; Stamm, M. *Prog. Org. Coat.* **2006**, *55*, 168.
(17) Zhang, Z.; Vaisocherova, H.; Cheng, G.; Yang, W.; Xue, H.; Jiang, S. *Biomacromolecules* **2008**, *9*, 2686.
(18) Pasche, S.; De Paul, S. M.; Vörös, J.; Spencer, N. D.; Textor, M. *Langmuir* **2003**, *19*, 9216.
(19) Perry, S. S.; Yan, X.; Limpoco, F. T.; Lee, S.; Müller, M.; Spencer, N. D. *ACS Appl. Mater. Interfaces* **2009**, *1*, 1224..
(20) Jiang, S.; Cao, Z. *Adv. Mater.* **2010**, *22*, 920.
(21) Ladd, J.; Zhang, Z.; Chen, S.; Hower, J. C.; Jiang, S. *Biomacromolecules* **2008**, *9*, 1357.
(22) Matyjaszewski, K.; Xia, J. H. *Chem. Rev.* **2001**, *101*, 2921.
(23) Fu, L.; Chen, X.; He, J.; Xiong, C.; Ma, H. *Langmuir* **2008**, *24*, 6100.
(24) Nakayama, Y.; Matsuda, T. *Macromolecules* **1999**, *32*, 5405.
(25) Kim, J.-B.; Huang, W.; Bruening, M. L.; Baker, G. L. *Macromolecules* **2002**, *35*, 5410.
(26) Kim, J.-B.; Huang, W.; Miller, M. D.; Baker, G. L.; Bruening, M. L. *J. Polym. Sci., Part A: Polym. Chem.* **2003**, *41*, 386.
(27) Prucker, O.; Rühe, J. *Macromolecules* **1998**, *31*, 602.
(28) Matyjaszewski, K.; Paik, H.-j.; Zhou, P.; Diamanti, S. J. *Macromolecules* **2001**, *34*, 5125.
(29) Nanda, A. K.; Matyjaszewski, K. *Macromolecules* **2003**, *36*, 1487.